Randomly gapped wall stabilization for time-dependent magnetic confinement fields

Paul M. Bellan

California Institute of Technology, Pasadena, California 91125
(Received 24 July 1980; accepted 6 February 1981)

An azimuthally continuous conducting wall cannot be used to provide stabilization for time-dependent magnetic confinement fields, such as the recently proposed traveling, compressing mirror [P. M. Bellan, Phys. Rev. Lett. **43**, 858 (1979)], because, unlike static confinement fields, time-dependent confinement fields cannot penetrate such a wall. If the wall has a gap, then time-dependent fields can penetrate, but the gap produces an azimuthal asymmetry of the field which can cause enhanced particle losses. By splitting the wall into a large number of short insulated axial sections, each with a randomly oriented azimuthal gap, (i) the time-dependent confining field can penetrate the wall, (ii) wall stabilization is obtained, and (iii) azimuthal symmetry is maintained.

I. INTRODUCTION

Fusion reactors employing field-reversed configurations (e.g., plasma-confining ion rings[1] or field-reversed plasmas[2]) offer the advantages of both mirrors and tokamaks; i.e., simple external coil systems and closed field lines, respectively. Furthermore, because external traveling magnetic mirrors could be used to translate the field-reversed configuration through distinct, linearly segmented, coaxial reactor sections, the reactor could be split into several such sections, each optimized for a particular process (e.g., plasma or ring generation, fueling, heating, thermonuclear burning, exhaust) of the operating cycle. By having several rings or plasmas in the reactor at once, all these processes could occur simultaneously so as to provide optimum utilization of each reactor section.

A scheme for producing traveling magnetic mirrors in a particularly simple way has recently been proposed by the author.[3] Besides being simple, the scheme also provides the possibility of three-dimensional, constant-field-energy adiabatic compression of the magnetic mirror, and, hence, compression and heating of the mirror-confined plasma or ring. Figure 1 shows the main elements of this scheme. The traveling mirror is produced by a double-hump current impulse [left, Fig. 1(a)] propagating in wave-like fashion along a macroscopic delay line. This delay line is a long solenoid, the coils of which are connected to capacitors [right, Fig. 1(a)]. Three-dimensional adiabatic compression is achieved by gradually decreasing the bore and intercoil spacing of successive coils, while increasing their respective turns number [Fig. 1(b)], so that the characteristic mirror-wave propagation velocity decreases causing both a WKB[4] steepening of the mirror field (perpendicular compression) and an axial contraction (parallel compression). Figure 2 shows an example of traveling mirror compression observed on a 2.5 m long table-top compressor; the magnetic field increases by 30× and the field volume decreases by 10^3 on this device. Large compression ratios are readily obtained with this scheme and, because the wave energy, i.e., $\int B^2\,dr$ is constant (neglecting particle diamagnetism), compression occurs without any energy input beyond the initial field energy. Thus, unlike conventional (i.e., fixed field geometry) compression schemes where $\int B^2\,dr$ increases as B^2, large[5] compression and heating factors can be obtained with modest initial energies. (The importance of decreasing field volume has previously been noted by Coensgen *et al.*[5])

In Ref. 3 it was proposed to use the traveling magnetic mirror to compress either reversed-field particle rings[6] or reversed-field plasmas.[7] However, in order for this to succeed for rings, the dissipative precessional instability[8] must be prevented, while for plasmas, the radially shifting instability (an $m=1$ magnetohydrodynamic mode[9] in which the whole plasma becomes radially displaced as a rigid body) must be prevented. Both these instabilities are caused by the fact that a simple mirror field has $\partial B_z/\partial\rho < 0$ (here, B_z is the axial magnetic field and ρ is the radial distance from the axis of symmetry of the mirror field). Consequently, the magnetic moment potential energy $\mu \cdot B$ of a ring or plasma has the shape of a potential "hill" with a maximum at $\rho=0$, so that radial displacements

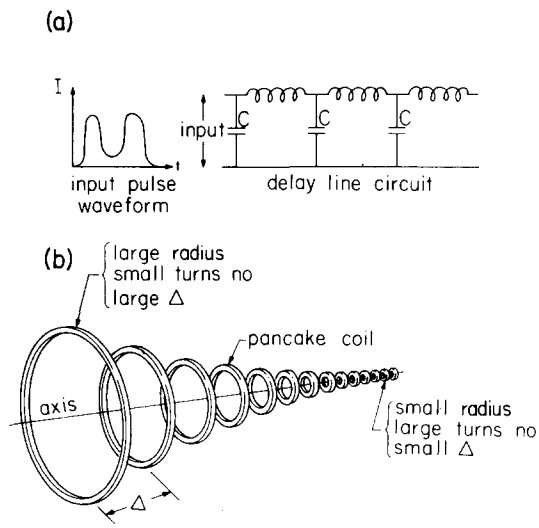

FIG. 1. Traveling mirror adiabatic compressor: (a) Left, input to solenoid delay line; right, circuit of solenoid delay line. (b) Coil geometry of solenoid delay line compressor.

 0031-9171/81/050947-09$00.90

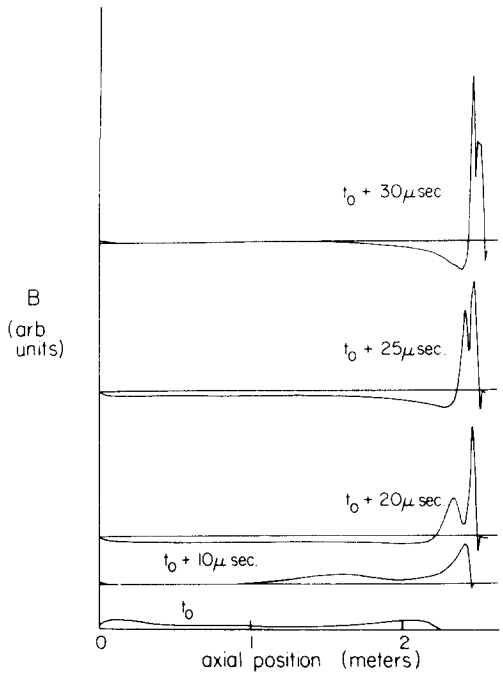

FIG. 2. Typical observed progagating, compressing mirror field on a 2.5 m long table-top compressor. Initial coil bore radius = 1.25 cm, final (compressed) coil bore radius = 0.2 cm.

of the ring or plasma are unstable. The actual dynamics of the plasma instability (simple radial motion) differ from the ring instability (unstable precession), but the ultimate result (radial expulsion) is the same. The established ways of preventing both these instabilities are wall stabilization or quadrupole field stabilization[10,11]; in the next paragraph these stabilization methods will be shown to be incompatible with the scheme proposed in Ref. 3.

For wall stabilization of static mirror fields, an external cylindrical conducting wall, coaxial with the mirror field, is placed around the ring (in the following, ring is taken to mean ring or plasma). When the instability displaces the ring, wall image currents induced by the motion of the ring generate a stabilizing restoring force.[12-14] This image-produced restoring force is proportional to the square of the ring current, whereas the destabilizing force [i.e., $\partial(\mu \cdot B)/\partial\rho$] is linearly proportional to the ring current, so that there is a minimum ring current for wall stabilization to work. Onset of the precessional instability when the ring current decays below this minimum has been clearly observed[15] in wall-stabilized reversed-field electron ring experiments at Cornell; detailed calculations of the minimum by Woodall *et al.*[14] for a variety of ring geometries have shown excellent agreement with the experimental observations.

For quadrupole stabilization, external conductors (Ioffe[10] bars) parallel to the axis of symmetry are added to the mirror field. Currents in these conductors generate a quadrupole field that is strongest near the conductors so that when the ring tries to "fall down" the $\mu \cdot B$ potential hill, it is pushed back by the quadrupole field. Quadrupole stabilization has been demonstrated to work well with non-field-reversed plasmas (to the author's knowledge, it has not been attempted on field-reversed plasmas). For reversed-field rings, however, Luckhardt and Fleischmann[16] have observed that, while quadrupole fields do stabilize, they also greatly enhance particle losses. Cohen *et al.*[17] have shown that these enhanced losses come from the non-axisymmetry of the quadrupole fields and that, in particular, the typical $m = 1$ or 2 azimuthal dependence of the quadrupole field drives a higher order orbital resonance of the particles in the ring. Consequently, quadrupole fields are unsuitable for field-reversed rings, but may be suitable for stabilizing field-reversed plasmas (Boozer[18] has shown that, for plasmas, arbitrarily small quadrupole perturbations open up the field lines, but that if the plasma pressure exceeds the perturbation field pressure, the plasma diamagnetic current distorts the magnetic perturbation and can overcome the effect of the open lines).

The methods given here cannot be used to stabilize the traveling (i.e., time-dependent) mirror of Ref. 3 for the following reasons: Conventional wall stabilization will not work because an azimuthally continuous wall prevents field lines of the time-dependent traveling mirror from penetrating the wall. Quadrupole stabilization might work for field-reversed plasmas, but would cause excessive particle losses for reversed-field rings. A propagating quadrupole synchronous with the traveling mirror might be arranged by putting Ioffe-like windings electrically in series with the solenoid coils, but this would be cumbersome. Hence, neither of the conventional stabilization schemes are suitable for the traveling mirror compressor. This paper describes a new stabilization scheme, namely, randomly gapped wall stabilization (a modification of conventional wall stabilization), that will stabilize the traveling mirror without introducing

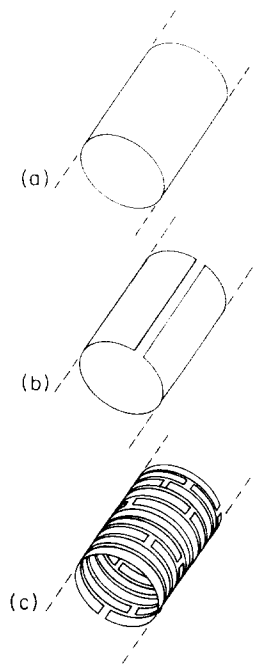

FIG. 3. Wall configurations; (a) ungapped; (b) simple gapped; (c) randomly gapped.

any of these problems. This scheme could also provide stabilization for other time-dependent magnetic field configurations (e.g., theta pinches) where ungapped walls would prevent field penetration.

Section II reviews stabilization of the precessional instability[8] in a static mirror field by an azimuthally continuous [cf. Fig. 3(a)], perfectly conducting wall,[12-14] and discusses the wall currents associated with the two, i.e., static and dynamic, wall-produced stabilizing terms. Section III A shows that if the wall is slit parallel to the z axis to form a gap [cf. Fig. 3(b)] so as to allow the traveling mirror field to penetrate inside the wall, the dynamic stabilizing term is unaffected while the static stabilizing term disappears. Section III A also shows that, because the gap is at a specific azimuthal angle, the fields associated with this simple gapped wall are not axisymmetric and so will cause particle losses as with quadrupoles. Section III B shows that if the wall is split into short axial sections, each with a gap oriented at a random azimuthal angle [cf. Fig. 3(c)], then the fields become axisymmetric. This configuration also provides the dynamic stabilization term and allows the traveling mirror to penetrate inside. Thus, this randomly gapped wall provides exactly what is needed to stabilize the traveling mirror field. Section IV describes the results of a very simple table-top experiment which verifies the analysis of Sec. III. In Sec. V a brief summary is given.

II. REVIEW OF WALL STABILIZATION OF PRECESSIONAL INSTABILITY IN STATIC MIRROR FIELDS

Conventional (i.e., no gap) wall stabilization of the precessional instability in a static mirror field is briefly reviewed here in order to introduce the geometry, the physical phenomena, the notations, and the mathematical methods that will be used in Sec. III. Section II A reviews the precessional instability in the presence of a prescribed wall field B_{z1}^{w}, while Sec. II B reviews how this wall field is calculated.

A. Precessional instability[8]

Consider the axis-encircling ring as a rigid "superparticle" gyrating in the midplane of an externally produced static magnetic mirror field $B_z^e(\rho) = B_0(1 - \frac{1}{2}n\rho^2/\rho_0^2)$, where B_0 is the axial field on the axis of symmetry at the midplane; the field index n is a measure of the mirror field curvature at the equilibrium gyroradius ρ_0 of the particle; and cylindrical coordinates ρ, θ, and z are used. Furthermore, there is a perfectly conducting thin wall of radius b ($b > \rho_0$) coaxial with the mirror field; this wall is azimuthally continuous and symmetric (i.e., no gaps) as in Fig. 3(a). Image currents in the wall generate a field $B_z^w(\rho)$ which acts on the particle through the Lorentz force.

Now suppose, as Fig. 4 shows, that the particle gyrocenter is displaced from the mirror axis of symmetry by a small vector ξ, where ξ makes an angle ϕ with respect to the x axis of the mirror field coordinate system (recall that θ is measured relative to this x axis). This situation occurs when the particle is precessing, in which case the vector ξ slowly rotates at the precession frequency ω_p about the mirror axis. Define a second cylindrical coordinate system ρ^*, θ^*, z with axis of symmetry passing through the particle gyrocenter. The two coordinate systems are related by

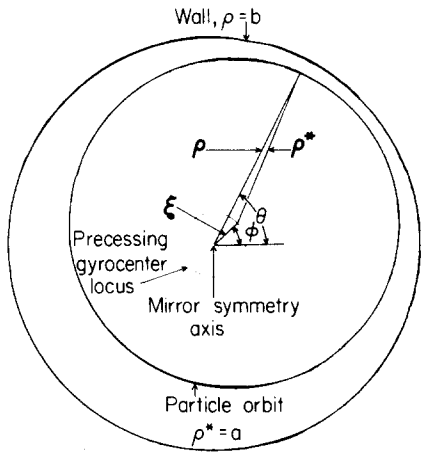

FIG. 4. Geometry of precessing particle, mirror symmetry axis, and wall.

$$\rho^* = \rho - \xi ,$$

so that

$$\rho^* = \rho - \xi\cos(\phi - \theta) . \tag{1}$$

In a time short compared with the precessional period, but long compared with the gyro-period, the particle gyro-radius is $\rho^* = a \simeq \rho_0$. Thus, in the mirror coordinate system the particle orbit is

$$\rho(\theta) = a + \xi\cos(\phi - \theta) .$$

In Ref. 8 the precession frequency is found [from a dispersion relation involving the displacement $\xi\cos(\phi - \theta)$, and the associated perturbation in the magnetic field seen by the particle] to be

$$\omega_p = -\frac{1}{2}\frac{a}{\xi\cos(\phi - \theta)}\frac{B_{z1}}{B_0}\omega_c , \tag{2}$$

where ω_c is the cyclotron frequency and B_{z1} is the magnetic field perturbation seen by the particle at its displaced position. In general, $B_{z1} = B_{z1}^e + B_{z1}^w$, where B_{z1}^e results from the radial gradient of the external mirror field and B_{z1}^w from image currents in the wall. The mirror component is just $B_{z1}^e = \rho_1 \partial B_z^e/\partial\rho = -[\xi\cos(\phi - \theta)]nB_0/a$; B_{z1}^w will be calculated in Sec. II B.

Reference 8 also shows that if there are frictional forces acting on the precessional motion, then the precession will grow (or possibly damp) with growth rate

$$\gamma = \frac{1}{2}\frac{\omega_p}{\omega_c}\frac{\mathcal{F}}{m} , \tag{3}$$

where $\mathcal{F}$ is the sum of the θ- and ρ-directed frictional forces, and m is the mass of the particle. Equation (3) shows that unstable precession occurs if $\omega_p > 0$. If there is no wall, then $B_{z1} = B_{z1}^e$ giving $\omega_p = \frac{1}{2}n\omega_c$ showing that a simple mirror is unstable; from Eq. (3) the instability growth rate is proportional to n.

B. Ungapped wall stabilization

Now, assume that there is an azimuthally continuous [as in Fig. 3(a)] wall at $\rho = b$. The only currents are the ring current and the wall image currents; i.e., there are no volume currents. Thus, everywhere except on the wall and on the ring $\boldsymbol{B} = \nabla\psi$, where ψ consists of linear combinations of $I_m(k\rho)\exp(im\theta + ikz)$, and $K_m(k\rho)\exp(im\theta + ikz)$ (here, I_m and K_m are modified Bessel functions). Let us write $\psi = \psi^r + \psi^w$, where ψ^r is the component that would be generated by the ring if there were no wall, and ψ^w is the component generated by the wall which, when added to ψ^r, satisfies the boundary conditions at the wall. Since I_m diverges at infinity, while K_m diverges at the origin, ψ^w has only $K_m(k\rho)$ terms for $\rho > b$ and only $I_m(k\rho)$ terms for $\rho < b$. Similarly, the ring generates only $K_m(k\rho^*)$ terms for $\rho^* > a$ and only $I_m(k\rho^*)$ terms for $\rho^* < a$. Starred coordinates are used for the ring because its symmetry axis is its gyrocenter, not the mirror symmetry axis. Because the ring is azimuthally symmetric, it generates only $m = 0$ modes.

Let us suppose the ring has an axial surface current distribution $j_\theta(z)$ and define $\tilde{j}_\theta(k)$ as the z-Fourier transform of $j_\theta(z)$. Since the equations are linear, each k mode must satisfy the boundary conditions at the ring and at the wall. These boundary conditions are; (i) there is a jump in B_z at the ring corresponding to the current on the ring, (ii) B_ρ is continuous across the ring, (iii) B is zero in the wall, and (iv) B_ρ is continuous across the wall-vacuum interface. Since a static mirror field is assumed here, these boundary conditions involve only ψ^r and ψ^w. The $\tilde{\psi}^r(k)$ satisfying (i) and (ii) is

$$\tilde{\psi}^r(k) = \begin{cases} -i\mu_0\tilde{j}_\theta(k)aK_0'(ka)I_0(k\rho^*), & \rho^* < a, \\ -i\mu_0\tilde{j}_\theta(k)aI_0'(ka)K_0(k\rho^*), & \rho^* > a, \end{cases} \tag{4}$$

where μ_0 is the permeability of free space. Boundary conditions (iii) and (iv) combine to give $B_\rho = 0$ at both the wall interior and exterior surfaces. Expressing ψ^r in the unstarred coordinates this condition becomes

$$\frac{\partial\tilde{\psi}^w}{\partial\rho}\Big|_{\rho=b} - i\mu_0\tilde{j}_\theta(k)kaI_0'(ka) \times[K_0'(kb) - k\xi\cos(\phi-\theta)K_0''(kb)] = 0. \tag{5}$$

The appropriate interior ψ^w satisfying Eq. (5) is

$$\tilde{\psi}^w(k) = -i\mu_0\tilde{j}_\theta(k)a[\alpha_1^w(k)I_0(k\rho) + \alpha_1^w(k)I_1(k\rho)\cos(\phi-\theta)], \tag{6}$$

where

$$\alpha_0^w(k) = -I_0'(ka)K_0'(kb)/I_0'(kb), \tag{7a}$$

$$\alpha_1^w(k) = k\xi I_0'(ka)K_0''(kb)/I_1'(kb). \tag{7b}$$

Equations (7a) and (7b) give the midplane wall axial field as

$$B_z^w(\rho,\theta,z) = -\mu_0 a\int dk\, k\tilde{j}_\theta(k)I_0'(ka)\left(\frac{K_0'(kb)}{I_0'(kb)}I_0(k\rho) - k\xi\cos(\phi-\theta)\frac{K_0''(kb)}{I_1'(kb)}I_1(k\rho)\right). \tag{8}$$

For Eqs. (2) and (3) the time-dependent wall field at the displaced ring position is required; i.e., the field at $\rho = a + \xi\cos(\phi-\theta)$. Keeping only terms first order in ξ gives

$$B_{z1}^w = \mu_0 a\xi\cos(\phi-\theta)\int dk\, k^2\tilde{j}_\theta(k)[I_1(ka)]^2 \times\left(\frac{K_1(kb)}{I_1(kb)} - \frac{K_1'(kb)}{I_1'(kb)}\right). \tag{9}$$

The first term in the integrand of Eq. (9) is known as the static stabilization term, the second as the dynamic stabilization term; these terms have comparable magnitudes. Combining Eq. (9) with the perturbed mirror field and inserting in Eqs. (2) and (3) shows stability exists if

$$\frac{\mu_0}{B_0}\int dk\,\tilde{j}_\theta(k)(ka)^2[I_1(ka)]^2\left(\frac{K_1(kb)}{I_1(kb)} - \frac{K_1'(kb)}{I_1'(kb)}\right) > n, \tag{10}$$

which is just the "nonaveraged" result of Woodall *et al.*[14]

Now consider the wall currents that are associated with the wall field. Because both the wall and the ring have K_m dependence for $\rho > b$ and the exterior wall field is chosen to satisfy $B_\rho = 0$ at the wall exterior surface, the wall field must exactly cancel the ring field everywhere in the region $\rho > b$; i.e., there is no net field outside the wall. The wall current is given by the jump in B at the wall; in particular, the θ component of the wall current is given by the jump in B_z, the z component by the jump in B_θ. The first term of Eq. (6) together with the $m = 0$ ring term provide an azimuthal current in the wall, which gives the static stabilization term; if the wall is slit as described in Sec. I, this current will be interrupted. The second term in Eq. (6) together with the corresponding ring field, provide an $m = 1$ current which gives the dynamic stabilization term. This second current has both θ and z components with $j_\theta \sim \cos(\phi-\theta)$ and $j_z \sim \sin(\phi-\theta)$. As shown in Fig. 5, these $m = 1$ currents will not be affected if the wall is slit, because new opposing currents on either side of the gap will provide separate return paths for each segment of the original current path (not possible for the $m = 0$ current). Consequently, the results of the next section may be anticipated: the dynamic stabilizing term remains when the wall is gapped, but the static stabilizing term disappears.

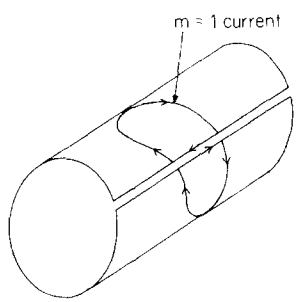

FIG. 5. $m = 1$ wall current on inside of gapped wall; since currents parallel to gap are adjacent and oppositely directed, they generate no net field.

III. RANDOMLY GAPPED WALL STABILIZATION OF TRAVELING MIRRORS

Transient axial magnetic fields can penetrate a gapped wall [cf. Fig. 3(b)], because no azimuthally directed axisymmetric currents can flow in such a wall (this is the basis of the flux concentrator,[19] which is just a thick gapped wall). Hence, a gapped wall coaxial with and inside the solenoid delay line of Ref. 3 will permit penetration by the traveling mirror wave.

In Sec. III A the fields of the simple gapped wall of Fig. 3(b) will be derived; these will be shown to have a preferred azimuthal direction determined by the azimuthal location of the gap. Such deviation from azimuthal symmetry can be expected to cause high order resonant interactions with particle orbits as was the case for quadrupole stabilization, and will probably cause similar enhanced particle losses. In Sec. III B the fields of the randomly gapped wall of Fig. 3(c) will be derived; these will be shown to provide stabilization without introducing azimuthal asymmetries. Hence, randomly gapped walls stabilize without destroying azimuthal symmetry and, as with simple gapped walls, permit penetration by the traveling (i.e., transient) mirror field.

The derivations in Sec. III A and III B are based on there being a new (and quite different) boundary condition at the gapped wall. This new boundary condition stems from the fact that field lines can penetrate through the gap (thus, the boundary condition, $B_\rho = 0$ at the wall, used in Sec. II is no longer valid).

A. Simple gapped wall

Without loss of generality assume the gap is at $\theta = 0$. The gap does not affect the ring current so that ψ^r is again given by Eq. (4). The new wall boundary condition can be seen by considering Fig. 6. Here, ϵ represents the azimuthal width of the gap and L is the axial extent of a short wall section. Since $B_\rho = 0$ on the conducting surface, B_ρ can only be finite in the gap. From Gauss' theorem the total flux (shown by arrows in Fig. 6) through the gap and the two cylinder end faces is zero, i.e.,

$$B_\rho^g \epsilon L + \int_0^b \int_0^{2\pi} [B_z(\rho, \theta\ z + L) - B_z(\rho, \theta, z)]\rho\, d\rho\, d\theta = 0,$$

or

$$B_\rho^g = -\frac{1}{\epsilon} \int_0^b \int_0^{2\pi} \frac{\partial B_z}{\partial z} \rho\, d\rho\, d\theta,$$

where B_ρ^g is the radial field through the gap. Here, B_ρ^g, B_z are each *net* field components resulting from the *sum* of the ring field, the external time-dependent mirror field, and the wall field. Now, $\epsilon = b\Delta\theta$, where $\Delta\theta$ is the angular width of the gap and B_ρ^g is finite only at the gap. By letting $\epsilon \to 0$ we can replace $1/\epsilon$ is this equation by $\delta(\theta)/b$, so that this gapped wall boundary condition becomes

$$B_\rho(b, \theta, z) = -\frac{\delta(\theta)}{b} \int_0^b \int_0^{2\pi} \frac{\partial B_z}{\partial z} \rho\, d\rho\, d\theta,$$

or

$$B_\rho^r(b, \theta, z) + B_\rho^e(b, \theta, z) + B_\rho^w(b, \theta, z) = -\frac{\delta(\theta)}{b} (g^r + g^e + g^w), \tag{11}$$

where

$$g^{r,e,w} = \int_0^{2\pi} \int_0^b \frac{\partial^2 \psi^{r,e,w}}{\partial z^2} \rho\, d\rho\, d\theta, \tag{12}$$

and r, e, w refer to ring, external mirror, and wall fields, respectively. Equation (11) is the basic equation to be solved in this section. Both the external mirror fields and ring fields are prescribed (the ring field is determined as in Sec. II by the jump condition at the ring), while the wall field (which occurs on both sides of the equation) is to be determined.

The method for finding the wall field, or equivalently ψ^w, is the following: ψ^w is expressed as a sum of linearly independent cylindrical solutions to Laplace's equation having unknown coefficients [cf. Eq. (6) for the comparable ungapped wall case]. B_ρ^w and g^w are evaluated in terms of these unknown coefficients, while B_ρ^r, B_ρ^e, g^r, and g^e are evaluated in terms of the prescribed fields. Substituting into Eq. (11) gives a set of equations for the unknown coefficients. Solving these equations determines the coefficients and so ψ^w and B^w. Because of the delta function in Eq. (11), all azimuthal harmonics in ψ^w must be retained; hence,

$$\tilde{\psi}^w = -i\mu_0 \tilde{j}_\theta(k) a \left(\sum_m \alpha_m^w(k) I_m(k\rho) \exp(im\theta) + \alpha_1^{w*} I_1(k\rho) \cos(\phi - \theta) \right), \quad \rho < b, \tag{13a}$$

$$\tilde{\psi}^w = -i\mu_0 \tilde{j}_\theta(k) a \left(\sum_m \beta_m^w(k) K_m(k\rho) \exp(im\theta) + \beta_1^{w*} I_1(k\rho) \cos(\phi - \theta) \right), \quad \rho > b. \tag{13b}$$

For later convenience, the terms proportional to the ring displacement have been written explicitly, and their (unknown) coefficients denoted by α_1^{w*}, β_1^{w*}. The terms in Eq. (11) will now be calculated.

Only $m = 0$ wall modes contribute to g^w so that

$$\tilde{g}^w = 2\pi i \mu_0 \tilde{j}_\theta(k) a \alpha_0^w(k) k b I_0'(kb). \tag{14}$$

The external mirror field (i.e., the traveling mirror which gives B_z^e) has the following magnetic potential:

$$\tilde{\psi}^e = -i\mu_0 \tilde{j}_\theta(k) a \alpha_0^e(k) I_0(k\rho), \tag{15}$$

here,

$$\alpha_0^e(k) = \tilde{j}_\theta^e(k) d K_0'(kd) / \tilde{j}_\theta(k) a,$$

where $\tilde{j}_\theta^e(k)$, d are, respectively, the mirror coil current

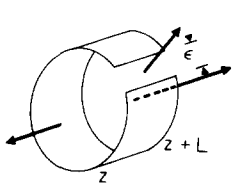

FIG. 6. Arrows indicate surfaces (i.e., gap and cylinder end faces) from which flux emanates when wall is gapped.

distribution and radius so that

$$\tilde{g}^e = 2\pi i \mu_0 \tilde{j}_\theta(k) a \alpha_0^e(k) k b I_0'(kb) . \tag{16}$$

Splitting the g^r integral into $0<\rho<a$ and $a<\rho<b$ parts and using Eq. (4), gives

$$\tilde{g}^r = i\mu_0 \tilde{j}_\theta(k) a k^2 \int_0^{2\pi} d\theta \Big(K_0'(ka) \int_0^a I_0(k\rho)\rho\, d\rho + I_0'(ka) \int_a^b K_0(k\rho)\rho\, d\rho + \mathcal{O}[\xi\cos(\phi-\theta)] \Big),$$

where the third term in the integral comes from the arguments of I_m, K_m being ρ^* and not ρ and also from the split between the inner and outer parts occurring at $a+\xi\cos(\phi-\theta)$ and not at a. This third term vanishes upon θ integration so that

$$\tilde{g}^r = i\mu_0 \tilde{j}_\theta(k) a 2\pi k b I_0'(ka) K_0'(kb) . \tag{17}$$

Substituting for $g^{r,e,w}$ in Eq. (11) and using

$$\delta(\theta) = (2\pi)^{-1} \sum_m \exp(im\theta) ,$$

gives the wall boundary condition as

$$\begin{aligned} &\tilde{B}_\rho^r(b,\theta,k) + \tilde{B}_\rho^e(b,\theta,k) + \tilde{B}_\rho^w(b,\theta,k) \\ &\quad = -i\mu_0 \tilde{j}_\theta(k) k a \{ [\alpha_0^w(k) + \alpha_0^e(k)] I_0'(kb) \\ &\qquad + I_0'(ka) K_0'(kb) \} \sum_m \exp(im\theta) . \end{aligned} \tag{18}$$

We can now substitute for the terms on the left-hand side of Eq. (18) by using Eqs. (4), (13a), and (15); this will give the desired set of equations for the α_m^w [the outer solution coefficients β_m^w are found by using Eq. (13b) instead of Eq. (13a); however, the β_m^w are not needed for the stability analysis and so will not be evaluated here]. Thus,

$$\begin{aligned} &I_0'(ka)[K_0'(kb) - k\xi\cos(\phi-\theta)K_0''(kb)] + \alpha_0^e(k) I_0'(kb) \\ &\quad + \sum_m \alpha_m^w(k) I_m'(kb)\exp(im\theta) + \alpha_1^{w*} I_1'(kb)\cos(\phi-\theta) \\ &\quad = \{ [\alpha_0^w(k) + \alpha_0^e(k)] I_0'(kb) \\ &\qquad + I_0'(ka) K_0'(kb) \} \sum_m \exp(im\theta) . \end{aligned} \tag{19}$$

The $m=0$ terms of Eq. (19) give an identity and leave α_0^w undetermined; however, it is clear that $\alpha_0^w = 0$, otherwise there would be a jump in the $m=0$ wall-produced axial field corresponding to an $m=0$ azimuthal current, which would be inconsistent with there being a gap. For $m=1$ we must consider both α_1^w and α_1^{w*}; α_1^w balances the $m=1$ term on the right-hand side of Eq. (19), while α_1^{w*} balances the $m=1$ [i.e., the $k\xi\cos(\phi-\theta)$ term] on the left-hand side. Solving for α_1^w gives

$$\alpha_1^w(k) = [\alpha_0^e(k) I_0'(kb) + I_0'(ka) K_0'(kb)] / I_1'(kb) ; \tag{20}$$

solving for α_1^{w*} gives

$$\alpha_1^{w*}(k) = k\xi I_0'(ka) K_0''(kb) / I_1'(kb) . \tag{21}$$

Note that Eq. (21) corresponds to the dynamically stabilizing term in Eq. (9), so, as postulated at the end of Sec. II, this term still occurs when the wall has a gap. For $m>1$, the α_m^w are solved as for α_1^w giving

$$\alpha_m^w(k) = [\alpha_0^e(k) I_0'(kb) + I_0'(ka) K_0'(kb)] / I_m'(kb) . \tag{22}$$

Thus, Eq. (13a) with coefficients defined by Eqs. (20)–(22) gives the interior ψ^w which, together with ψ^r [Eq. (4)] and ψ^e [Eq. (15)], satisfies the gapped wall boundary condition [Eq. (11)]. The axial wall field is thus

$$\begin{aligned} B_z^w(k) = \mu_0 \tilde{j}_\theta(k) k a \Big(&\sum_m \alpha_m^w(k) I_m(k\rho)\exp(im\theta) \\ &+ \alpha_1^{w*}(k) I_1(k\rho)\cos(\phi-\theta) \Big) . \end{aligned} \tag{23}$$

For stability against the precessional mode, Eq. (23) must be evaluated at the ring position $\rho = a + \xi\cos(\phi-\theta)$. Thus, at the ring, to first order in ξ, the wall-produced image field is

$$\begin{aligned} B_z^w\big|_{\rho^*=a} = \mu_0 j(k) k a \Big(&\sum_m \alpha_m^w(k) I_m(ka)\exp(im\theta) \\ &+ k\xi\cos(\phi-\theta) \sum_m \alpha_m(k) I_m'(ka)\exp(im\theta) \\ &+ \alpha_1^{w*}(k) I_1(ka)\cos(\phi-\theta) \Big) . \end{aligned} \tag{24}$$

The last term in Eq. (24) is the desired dynamically stabilizing term. However, the first term is a sum of azimuthal harmonics of the sort produced by a quadrupole field, and as noted in Sec. I, this type of field has been shown experimentally[16] and theoretically[17] to cause enhanced particle losses. (This first term describes the azimuthal asymmetry or "bump" caused by the well-defined azimuthal location of the gap.)

Thus, a simple gapped wall does generate stabilizing image fields, but it also generates azimuthal field harmonics (i.e., a bump at the gap) which will destroy particle confinement. In Sec. IIIB, it will be shown that, by splitting the wall into axial segments each having a randomly oriented gap, these destructive azimuthal harmonics cancel (i.e., the bump is smeared out) without affecting the desired dynamically stabilizing term.

B. Randomly gapped wall

Suppose, as shown in Fig. 3(c), the wall is split into axial sections, each of length h and each having a randomly oriented gap at θ_p; the sections are separated by a small axial gap of width ϵ_z. h is chosen so that each particle passes a large number of gaps during each gyroperiod, i.e., $h \ll 2\pi v_z/\omega_c$, where v_z is the parallel thermal velocity of the particle. The wall boundary condition on the pth section is the same as Eq. (11) except that the δ-function peak is at θ_p rather than $\theta=0$; thus, for the pth section, the boundary condition is

$$B_\rho(b,\theta,z) = -\frac{\delta(\theta-\theta_p)}{b} \int_0^{2\pi}\int_0^b \frac{\partial B_z}{\partial z}\rho\, d\rho\, d\theta . \tag{25}$$

By applying Gauss' theorem to the thin cylinder of radius b and length ϵ_z between two sections, the boundary condition in the gap between the sections is

$$\begin{aligned} &\int_0^{2\pi} \epsilon_z B_\rho(b,\theta,z) b\, d\theta + \int_0^{2\pi}\int_0^b \epsilon_z \frac{\partial B_z}{\partial z}\rho\, d\rho\, d\theta = 0 , \\ &\text{or} \\ &\int_0^{2\pi} B_\rho(b,\theta,z) d\theta = -\frac{1}{b}\int_0^{2\pi}\int_0^b \frac{\partial B_z}{\partial z}\rho\, d\rho\, d\theta . \end{aligned} \tag{26}$$

Equation (26) is just the azimuthal integral of Eq. (25), so satisfying Eq. (25) will automatically satisfy Eq. (26).

By Fourier transforming Eq. (25) with respect to z we obtain

$$\frac{1}{2\pi}\int_{-\infty}^{\infty} dz\left(\frac{\partial\psi^r}{\partial\rho}+\frac{\partial\psi^e}{\partial\rho}+\frac{\partial\psi^w}{\partial\rho}\right)_{\rho=b}\exp(-ikz)$$
$$=\frac{-1}{2\pi b}\sum_p\left\{\int_{ph}^{(p+1)h} dz\,\delta(\theta-\theta_p)\left[\int_0^{2\pi}\int_0^b\left(\frac{\partial^2\psi^r}{\partial z^2}\right.\right.\right.$$
$$\left.\left.\left.+\frac{\partial^2\psi^e}{\partial z^2}+\frac{\partial^2\psi^w}{\partial z^2}\right)\rho\,d\rho\,d\theta\right]\exp(-ikz)\right\}. \quad (27)$$

Equation (27) is the randomly gapped version of Eq. (11); note that, because θ_p depends on axial position, the delta function cannot be moved outside the integral over z on the right-hand side of the equation. Since Eqs. (4) and (15) still give the ring and external mirror fields, while Eq. (13a) gave the general, undetermined wall field, the cross-section integral on the right-hand side of Eq. (27) [i.e., the term in brackets] is again given by Eqs. (14), (16), and (17). The left-hand side of Eq. (27) is identical to the left-hand side of Eq. (19), but the axial dependence of θ_p changes the right-hand side. Hence, Eq. (27) becomes

$$I_0'(ka)[K_0'(kb)-k\xi\cos(\phi-\theta)K_0''(kb)]+\alpha_0^e(k)I_0'(kb)+\sum_m\alpha_m^w(k)I_m'(kb)\exp(im\theta)+\alpha_1^{w*}(k)I_1'(kb)\cos(\phi-\theta)$$
$$=\sum_p\frac{1}{2\pi k\tilde{j}_\theta(k)}\int_{ph}^{(p+1)h}dz\int k'\,dk'\,\tilde{j}_\theta(k')\exp[i(k'-k)z]\{[\alpha_0^w(k')+\alpha_0^e(k')]I_0'(k'b)+I_0'(k'a)K_0'(k'b)\}\sum_m\exp[im(\theta-\theta_p)]. \quad (28)$$

If we define

$$Q_{p,m}(k',k)=\frac{k'\tilde{j}_\theta(k')}{2\pi k\tilde{j}_\theta(k)}\int_{ph}^{(p+1)h}dz\exp[-im\theta_p+i(k'-k)z],$$

then Eq. (28) becomes

$$I_0'(ka)[K_0'(kb)-k\xi\cos(\phi-\theta)K_0''(kb)]+\alpha_0^e(k)I_0'(kb)+\sum_m\alpha_m^w(k)I_m'(kb)\exp(im\theta)+\alpha_1^{w*}(k)I_1'(kb)\cos(\phi-\theta)$$
$$=\sum_m\exp(im\theta)\int dk'\{[\alpha_0^w(k')+\alpha_0^e(k')]I_0'(k'b)+I_0'(k'a)K_0'(k'b)\}\sum_p Q_{p,m}(k',k). \quad (29)$$

Now since θ_p is a random function of p

$$\sum_p Q_{p,m}(k',k)=0 \quad \text{if } m\neq 0$$

and

$$\sum_p Q_{p,m}(k',k)=\delta(k'-k) \quad \text{if } m=0,$$

so that, after some cancellations, Eq. (29) becomes

$$-k\xi\cos(\phi-\theta)I_0'(ka)K_0''(kb)$$
$$+\sum_m\alpha_m^w(k)I_m'(kb)\exp(im\theta)+\alpha_1^{w*}(k)I_1'(kb)\cos(\phi-\theta)$$
$$=\alpha_0^w(k)I_0'(kb), \quad (30)$$

which is similar to Eq. (19), except that there are no azimuthally dependent terms on the right-hand side. As in the simple gapped wall case [cf. discussion following Eq. (19)] α_0^w is undetermined by Eq. (30), but because the gap prevents $m=0$ currents from flowing, we set $\alpha_0^w=0$. However, unlike the simple gapped wall, for $m\neq 0$ all the α_m^w (except α_1^{w*}) also vanish. Thus, the wall field is given by

$$\tilde{\psi}^w(k,\rho,\theta)=-i\mu_0\tilde{j}_\theta(k)a\alpha_1^{w*}(k)I_1(k\rho)\cos(\phi-\theta),$$
$$\rho<b, \quad (31)$$

where α_1^{w*} is given by Eq. (21). Equation (31) corresponds to the second term of Eq. (6) which provided the second, i.e., dynamic stabilization, term of Eq. (9). Thus, for a randomly gapped wall, Eq. (10) is replaced by

$$-\frac{\mu_0}{B}\int dk(ka)^2\tilde{j}_\theta(k)[I_1(ka)]^2\frac{K_1'(kb)}{I_1'(kb)}>n. \quad (32)$$

Consequently, a randomly gapped wall preserves axisymmetry, allows the mirror field to penetrate, and provides the dynamically stabilizing term. Because a randomly gapped wall does not have the static stabilizing term, it provides somewhat less stabilizing effect than an ungapped wall (about a factor of two less, since

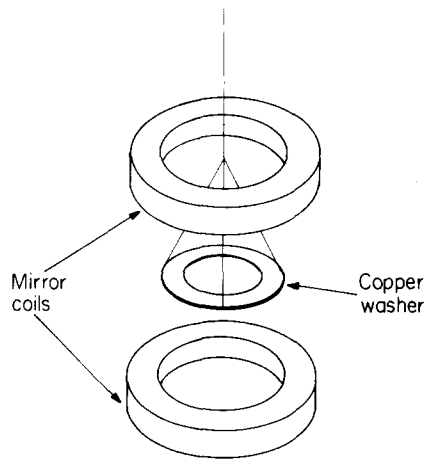

FIG. 7. Table-top demonstration experiment; when suspended washer is slightly displaced from symmetry axis it experiences outward $\mu\nabla B$ force. Randomly gapped wall (not shown) prevents this instability.

the static and dynamic terms have approximately equal magnitudes, cf. Fig. 4 of Woodall *et al.*[14]).

The wall image fields and currents produced by a plasma undergoing a radial shift instability (i.e., $m = 1$ magnetohydrodynamic rigid body mode) are exactly the same as the image fields and currents produced by a ring undergoing the precessional instability so that a randomly gapped wall will also provide stabilization for the radial shift mode of a plasma.

IV. TABLE TOP DEMONSTRATION OF RANDOMLY GAPPED WALL STABILIZATION

Figure 7 shows a sketch of a simple table top experiment which verifies the assertions of Sec. III. Here, two coils (each 270 turns of no. 16 wire, each 9 cm radius), spaced 15 cm apart, provide a simple mirror field. The coils are connected in parallel with a 1 μF, 3 kV capacitor to form a resonant circuit, with resonant frequency of 1.5 kHz. At resonance this circuit has an impedance of 2.5 kΩ and a Q of approximately 30. An audio amplifier (driven by a signal generator tuned to 1.5 kHz), connected to the circuit through an impedance-matching transformer, gives 600 A turns rms on each coil. The corresponding magnetic field at the center of the mirror is $B_z^e \sim 6\times10^{-3}$ T. A copper washer (o.d. 8.8 cm, i.d. 7.4 cm, thickness 0.2 cm, mass $M = 3\times10^{-2}$ kG, inductance ($L \sim 0.2$ μH) is suspended in the center of the mirror; the point of suspension is 1.7 m above the mirror center. Because the washer conserves flux, currents ($I \sim B_z^e \pi r^2/L \sim 100$ A rms) will flow in the washer and give it a magnetic moment $\mu = I\pi r^2 \sim 0.5$ A m^2 (here, r is the washer radius).

If the washer is exactly on the mirror symmetry axis, then the radial $\mu\nabla B$ forces azimuthally cancel [at the washer ∇B has order of magnitude approximately $B/$(distance from coils) or approximately 6×10^{-2} T/m]. However, if the washer is slightly displaced from the symmetry axis, these forces do not cancel and the washer, because it is diamagnetic, experiences a radially outward force. The washer will move radially outward until the magnetic torque $\mu\nabla B\times\mathbf{R} = \mu|\nabla B|R\cos\delta$ about the washer suspension point is balanced by the oppositely directed gravitational torque $M\mathbf{g}\times\mathbf{R} = MgR\sin\delta$ (here, R is the vector from the washer to the point of suspension and δ is the angle R makes relative to the vertical). This balance would occur at $\delta \simeq \mu|\nabla B|/Mg \simeq 6°$ or, as was the case here, when the suspending wire hits the inside of the upper coil. Thus, application of current to the coils causes the washer (when it is initially slightly displaced from the mirror symmetry axis) to swing to the side, in the direction of its initial displacement, until its support wire hits the inside of the upper coil (the washer moves about 4 cm, i.e., approximately 1.5°, in a fraction of a second).

A randomly gapped wall was constructed by stacking six slightly larger copper washers (o.d. 12.1 cm, i.d., 10.2 cm, thickness 0.2 cm), each having an azimuthal gap. The gaps were randomly oriented and thin Bakelite insulators separated the washers. The randomly gapped wall was placed around the suspended washer which was slightly displaced from the mirror symmetry axis, as before. The wall was arranged so that its center coincided with neither the mirror symmetry axis nor the suspended washer center. When power was applied to the mirror, the suspended washer moved to center itself in the randomly gapped wall, a clear indication of stabilization by the wall. Because of the very small damping in this system, the suspended washer initially overshot the wall center and then oscillated (oscillation amplitude$<\sim$0.5 cm) about the center with slowly decreasing amplitude until it came to rest at the center. During these oscillations the suspended washer never touched the wall, also a clear indication of wall stabilizing forces. When the wall was quickly removed (by lowering it), the suspended washer underwent the instability described here.

The instability of the suspended washer is similar in nature to both the precessional and the radial shift instabilities in that all are caused by a $\mu\nabla B$ force, and the wall stabilization fields and currents are identical for all three situations. Thus, this simple experiment confirms the results of Sec. III, namely, a randomly gapped wall (which can be axisymetrically penetrated by a time-dependent mirror field) will provide stabilization against the precessional and radial shift instabilities.

V. SUMMARY AND CONCLUSIONS

In order to stabilize a traveling (i.e., time-dependent) magnetic mirror against the precessional mode of rings or the radial shift mode of plasmas, it is necessary to have a stabilization scheme which (i) allows the transient mirror field to penetrate inside the stabilizing structure, and (ii) does not affect the mirror field axisymmetry. In Sec. III A it was shown that a simple gapped wall provides stabilization and allows penetration of the mirror field, but it destroys the axisymmetry. In Sec. III B it was shown that a randomly gapped wall (consisting of insulated axial segments, each with a randomly oriented azimuthal gap) provides stabilization, allows the mirror field to penetrate, and preserves axisymmetry. Section IV described a simple table top experiment which verified the stabilizing behavior of a randomly gapped wall. Thus a randomly gapped wall will provide stability for the traveling magnetic mirror described in Ref. 3. It could also be used in other situations (e.g., theta pinches) where axisymmetric wall stabilization is desired for a transient confining field.

ACKNOWLEDGMENT

Support by an Alfred P. Sloan Fellowship is gratefully acknowledged.

[1]H. H. Fleischmann and T. Kammash, Nuc. Fusion **15**, 1143 (1975).

[2]A. C. Smith, G. A. Carlson, H. H. Fleischmann, W. Grossman, Jr., T. Kammash, K. R. Schultz, and D. M. Woodall, in *Proceedings of the Third Symposium on Physics and Tech-*

nology of Compact Toroids in the Magnetic Fusion Energy Program (Los Alamos Scientific Laboratory, Los Alamos, New Mexico, 1980), p. 12.
[3]P. M. Bellan, Phys. Rev. Lett. **43**, 858 (1979).
[4]J. Mathews and R. L. Walker in *Mathematical Methods of Physics* (Benjamin, New York, 1965), p. 26.
[5]F. H. Coensgen, W. F. Cummins, A. W. Molvik, W. E. Nexsen, T. C. Simonen, and B. W. Stallard, in *Plasma Physics and Controlled Nuclear Fusion Research* (International Atomic Energy Agency, Vienna, 1975), Vol. I, p. 323.
[6]M. L. Andrews, H. Davitian, H. H. Fleischmann, B. Kusse, R. E. Kribel, and J. A. Nation Phys. Rev. Lett. **27**, 1428 (1971).
[7]C. W. Hartman, W. C. Condit, E. Granneman, D. Prono, A. C. Smith, Jr., J. Taska, and W. C. Turner, in *Proceedings of the International Conference on Plasma Physics* (Fusion Research Association of Japan, Nagoya, 1980), Vol. I, p. 34; T. R. Jarboe, I. Henins, H. W. Hoida, R. K. Linford, J. Marshall, D. A. Platts, and A. R. Sherwood, Phys. Rev. Lett. **45**, 1264 (1980).
[8]H. P. Furth, Phys. Fluids **8**, 2020 (1965).
[9]M. N. Rosenbluth and C. L. Longmire, Ann. Phys. **1**, 120 (1957).
[10]M. S. Ioffe and R. I. Sobolev, At. Energ. **17**, 366 (1964) [Sov. At. Energy **17**, 1112 (1964)].
[11]D. M. Woodall, H. H. Fleischmann, and H. L. Berk, Phys. Rev. Lett. **34**, 260 (1975).
[12]J. W. Beal, M. Brettschneider, N. C. Christofilos, R. E. Hester, W. A. Lamb, W. A. Sherwood, R. L. Spoerlein, P. S. Weiss, and R. E. Wright, in *Plasma Physics and Controlled Nuclear Fusion Research* (International Atomic Energy Agency, Vienna, 1969), Vol. I, p. 967.
[13]H. L. Berk and R. N. Sudan, J. Plasma Phys. **6**, 413 (1971).
[14]D. M. Woodall, R. V. Lovelace, R. A. Meger, H. H. Fleischmann, and H. L. Berk, Phys. Fluids **22**, 155 (1979).
[15]J. J. Bzura, T. J. Fessenden, H. H. Fleischmann, D. A. Phelps, A. C. Smith, Jr., and D. M. Woodall, Phys. Rev. Lett. **29**, 256 (1972).
[16]S. C. Luckhardt and H. H. Fleischmann, Phys. Rev. Lett. **39**, 747 (1977).
[17]R. H. Cohen, D. V. Anderson, and C. B. Sharp, Phys. Rev. Lett. **41**, 1305 (1978).
[18]A. H. Boozer, Nucl. Fusion **18**, 1663 (1978).
[19]M. N. Wilson and K. D. Srivastava, Rev. Sci. Instrum. **36**, 1096 (1965) and references therein.